



# DETECTION OF DIRECT CAUSAL EFFECTS AND APPLICATION TO EPILEPTIC ELECTROENCEPHALOGRAM ANALYSIS

ANGELIKI PAPANNA\* and DIMITRIS KUGIUMTZIS†  
*Department of Mathematical, Physical and Computational Sciences,  
Aristotle University of Thessaloniki, Thessaloniki, Greece*

\**agpapana@gen.auth.gr*

†*dkugiu@gen.auth.gr*

PÅL G. LARSSON

*Department of Neurosurgery, Oslo,  
Norway University Hospital, Oslo, Norway  
pal.gunnar.larsson@ous-hf.no*

Received December 31, 2010; Revised July 17, 2011

An extension of transfer entropy, called partial transfer entropy (PTE), is proposed to detect causal effects among observed interacting systems, and particularly to distinguish direct from indirect causal effects. PTE is compared to a linear direct causality measure, the Partial Directed Coherence (PDC), on known linear stochastic systems and nonlinear deterministic systems. PTE performs equally well as PDC on the linear systems and better than PDC on the nonlinear systems, both being dependent on the selection of the measure specific parameters. PTE and PDC are applied to electroencephalograms of epileptic patients during the preictal, ictal and postictal states, and PTE turns out to detect better changes of the strength of the direct causality at specific pairs of electrodes and for the different states.

*Keywords:* Granger causality; time series; information flow; transfer entropy; direct coherence.

## 1. Introduction

The identification of the information structure and the hidden dependencies among the observed components of complex dynamical systems is a difficult and challenging task. An even more difficult task is to distinguish between direct and indirect dependence or information flow. This problem is met in many applications and is of particular relevance for brain dynamics. Mapping the brain connectivity could be a major step in understanding the functions of the brain, and changes of the effective connectivity can possibly be taken as markers of

emerging pathological states, as in epilepsy [Schelter *et al.*, 2006a].

In the last decade, many nonlinear measures have been developed to estimate the strength and direction of coupling (also referred to as Granger causality or information flow) from an observed variable (or system)  $X$  to another observed variable  $Y$ . Among these measures, information-based measures, and transfer entropy (TE) [Schreiber, 2000] in particular, are found to be very effective in detecting the direction of information flow [Papanna & Kugiumtzis, 2008]. For direct Granger

---

† Author for correspondence

causality accounting for the presence of other variables, the existing measures are mostly linear, based on linear prediction models (conditioned or partial Granger causality index [Guo *et al.*, 2008]) and coherence (partial directed coherence, PDC [Baccala & Sameshima, 2001], and directed transfer function, dDTF [Blinowska *et al.*, 2004]).

Here, we extend TE and account for the presence of other variables in order to detect only direct information flow from  $X$  to  $Y$ , called Partial Transfer Entropy (PTE) (recently also developed in [Vakorin *et al.*, 2009]). We compare PTE to PDC, extensively used in brain connectivity, on time series from known stochastic and deterministic coupled systems. This study helps us interpret the results of the measures applied to epileptic electroencephalographic (EEG) records covering the preictal period (up to 3h prior to seizure onset), as well as the ictal (seizure) and postictal periods (minutes after the seizure). For example, we expect that the brain activity at the ictal state is different from before and after the seizure, which can be used for diagnostic purposes. Further, changes in brain connectivity at the preictal state can be used to form a seizure prediction tool. Another clinical use of causality measures can be the localization of the epileptic focus.

## 2. Methods

Transfer entropy (TE) quantifies the amount of information explained in  $Y$  at  $h$  time steps ahead from the state of  $X$  accounting for the concurrent state of  $Y$ . Given a bivariate time series  $\{x_t, y_t\}_{t=1}^n$  from the two systems, the states of  $X$  and  $Y$  at times  $t = (m-1)\tau + 1, \dots, n-h$  are defined by the state space reconstructed vectors  $\mathbf{x}_t = (x_t, x_{t-\tau}, \dots, x_{t-(m-1)\tau})'$  and  $\mathbf{y}_t = (y_t, y_{t-\tau}, \dots, y_{t-(m-1)\tau})'$ , respectively, where  $\tau$  is the delay time and  $m$  is the embedding dimension. Then TE from  $X$  to  $Y$  is defined as

$$\begin{aligned} \text{TE}_{X \rightarrow Y} &= -H(y_{t+h} | \mathbf{x}_t, \mathbf{y}_t) + H(y_{t+h} | \mathbf{y}_t) \\ &= -H(y_{t+h}, \mathbf{x}_t, \mathbf{y}_t) + H(\mathbf{x}_t, \mathbf{y}_t) \\ &\quad + H(y_{t+h}, \mathbf{y}_t) - H(\mathbf{y}_t), \end{aligned} \quad (1)$$

where  $H(x)$  is the Shannon entropy of the variable  $X$ .

Partial Transfer Entropy (PTE) extends TE to account for the presence of other interacting systems, collected in  $Z$ . Thus conditioning on  $\mathbf{z}_t$ , that

contains the state space reconstructed vectors of all observed variables of  $Z$ , only the direct causal effect of  $X$  to  $Y$  is measured by PTE, defined as

$$\begin{aligned} \text{PTE}_{X \rightarrow Y | Z} &= -H(y_{t+h} | \mathbf{x}_t, \mathbf{y}_t, \mathbf{z}_t) \\ &\quad + H(y_{t+h} | \mathbf{y}_t, \mathbf{z}_t). \end{aligned} \quad (2)$$

The estimation of TE and PTE relies on the estimation of the joint probability density functions in the expression of the entropies. For large dimension, the estimation of density functions can be problematic. For PTE and  $p$  observed variables, i.e.  $p-2$  observed variables of  $Z$ , the largest dimension for a joint distribution is  $mp+1$ , which can be prohibitively high for many probability density estimates. Thus, histogram-based estimates (discretizing the state space to equidistant or equiprobable intervals at each axis) are likely to fail even for small  $m, p$  and large  $n$ . We found that also estimates of kernel type making use of fixed bandwidths, such as the correlation sums, cannot provide reliable estimations for large dimensions [Papana & Kugiumtzis, 2009]. The latter estimate has been used to compute PTE in [Vakorin *et al.*, 2009], but dealing with small  $m$  and  $p$ . Here, we use the nearest neighbor estimate of the entropies [Kraskov *et al.*, 2004], which is found capable of handling best high dimension of the variables in the entropy terms [Vlachos & Kugiumtzis, 2010].

Linear measures of Granger causality are less sensitive to the dimension of the state variables. For model-based linear measures, the equivalent of the embedding dimension  $m$  is the order  $P$  of the autoregressive (AR) or Vector Autoregressive (VAR) model (assuming  $\tau = 1$ ). In this study, we compare PTE to Partial Directed Coherence (PDC), defined in terms of the Fourier transform of the coefficients of VAR regarding all  $p$  observed variables [Baccala & Sameshima, 2001]. Assuming for each variable vector at lag  $r$  the matrix of VAR coefficients  $\Phi(r)$ , the Fourier transform is  $A(f) = I - \sum_{r=1}^P \Phi(r) e^{-2i\pi fr}$  ( $I$  is the  $p \times p$  identity matrix), and PDC for the direct effect of variable (or component process)  $j$  to  $i$  at frequency  $f$  is defined as

$$\text{PDC}_{j \rightarrow i}(f) = \frac{|A_{ij}(f)|}{\sqrt{\sum_{l=1}^p |A_{lj}(f)|^2}}. \quad (3)$$

The final measure  $\text{PDC}_{j \rightarrow i}(P)$  is then defined as the average of  $\text{PDC}_{j \rightarrow i}(f)$  for all frequencies in a band

of interest, for the selected  $P$ .  $\text{PDC}_{j \rightarrow i}(P)$  measures the directed linear influence of variable  $j$  on variable  $i$  conditioned on the rest of the variables.

### 3. Application

#### 3.1. Simulated data

In all simulations we have three time series  $\{x_t, y_t, z_t\}_{t=1}^n$  of variables from each of the three coupled systems  $X$ ,  $Y$  and  $Z$  ( $p = 3$ ). We consider the three following interacting systems, each with the same interacting structure,  $X$  driving  $Y$  ( $X \rightarrow Y$ ) and  $Y$  driving  $Z$  ( $Y \rightarrow Z$ ).

**S1.** Three coupled autoregressive AR(1) models [Chen *et al.*, 2006]

$$\begin{aligned} x_t &= \theta_t, \\ y_t &= x_{t-1} + \eta_t, \\ z_t &= 0.5z_{t-1} + y_{t-1} + \epsilon_t \end{aligned}$$

where  $\theta_t$ ,  $\eta_t$ ,  $\epsilon_t$  are Gaussian white noise with zero mean and standard deviations 1, 0.2 and 0.3, respectively.

**S2.** Three coupled Henon maps

$$\begin{aligned} x_{t+1} &= 1.4 - x_t^2 + 0.3x_{t-1}, \\ y_{t+1} &= 1.4 - cx_t y_t - (1 - c)y_t^2 + 0.3y_{t-1}, \\ z_{t+1} &= 1.4 - cy_t z_t - (1 - c)z_t^2 + 0.3z_{t-1} \end{aligned}$$

with equal coupling strength  $c$  for  $X \rightarrow Y$  and  $Y \rightarrow Z$ , and  $c = 0, 0.05, 0.1, 0.2, 0.3, 0.4, 0.5$ .

**S3.** Three coupled Lorenz systems

$$\begin{aligned} \dot{x}_1 &= 10(y_1 - x_1) \\ \dot{y}_1 &= 28x_1 - y_1 - x_1 z_1 \\ \dot{z}_1 &= x_1 y_1 - \frac{8}{3} z_1, \\ \dot{x}_2 &= 10(y_2 - x_2) + c(x_1 - y_1) \\ \dot{y}_2 &= 28x_2 - y_2 - x_2 z_2 \\ \dot{z}_2 &= x_2 y_2 - \frac{8}{3} z_2, \\ \dot{x}_3 &= 10(y_3 - x_3) + c(x_2 - y_2) \\ \dot{y}_3 &= 28x_3 - y_3 - x_3 z_3 \\ \dot{z}_3 &= x_3 y_3 - \frac{8}{3} z_3 \end{aligned}$$

with equal coupling strength  $c$  for  $X \rightarrow Y$  and  $Y \rightarrow Z$ , and  $c = 0, 1, 2, 3, 4, 5$ . The second variable of each interacting system is observed.

For each system, and each  $c$  for systems S2 and S3, the direct causality measures PTE and PDC are computed for each ordered pair of the observed variables (six combinations) on 100 independent realizations to different initial conditions, and for  $n = 512, 1024, 2048, 4096, 8192$ . PTE is estimated for different number of neighbors  $k$  and embedding dimensions  $m$ , whereas PDC is estimated for different VAR orders  $P$  and for a range of frequencies in  $[0, 0.5]$ .

For the linear system S1, the simulation results showed that PTE performs equally well as PDC, both being positive for  $X \rightarrow Y$  and  $Y \rightarrow Z$  and zero for all other directed pairs. As Fig. 1 shows, the positive PDC values for the two direct causal effects are the same for  $P = 1$  and  $P = 2$ , whereas the PTE values for these two cases decrease when either the number of nearest neighbors  $k$  or the embedding dimension  $m$  increases, but only for small  $n$ . For small  $n$ , the PDC for some of the other pairs rises from the zero level when  $P$  changes from 1 to 2. However, in any case, a formal parametric significance test for PDC (see [Takahashi *et al.*, 2007; Schelter *et al.*, 2006b]) would only suggest the correct direct interaction, and the same is expected for PTE using surrogate data testing (e.g. see [Vlachos & Kugiumtzis, 2010]), as the variance of the measures is small. However, for larger parameter values, both measures have larger variance and the correct direct causal effects cannot be distinguished, especially for small  $n$ .

For the two nonlinear systems S2 and S3, PTE outperforms PDC. For appropriate selection of  $k$  and  $m$ , PTE gets large positive only for the two correct direct causal effects, and this holds even for small  $n$  and small coupling strengths  $c$ . On the other hand, PDC could not distinguish the two direct causal effects as the PDC values for other variable pairs were at the same level. Indicative results for PTE and PDC versus  $c$  are shown in Fig. 2 for system S2 and Fig. 3 for system S3. As shown in Figs. 3(b) and 3(c), the low performance of PDC is not due to the selection of  $P$ , and it persists even for large  $n$ . On the other hand, PTE performs properly even for small  $n$ , and moreover, the selection of appropriate parameters  $m$  and  $k$  improves the performance of PTE and increases the PTE values for the correct direct causal effects [see Figs. 2(a)

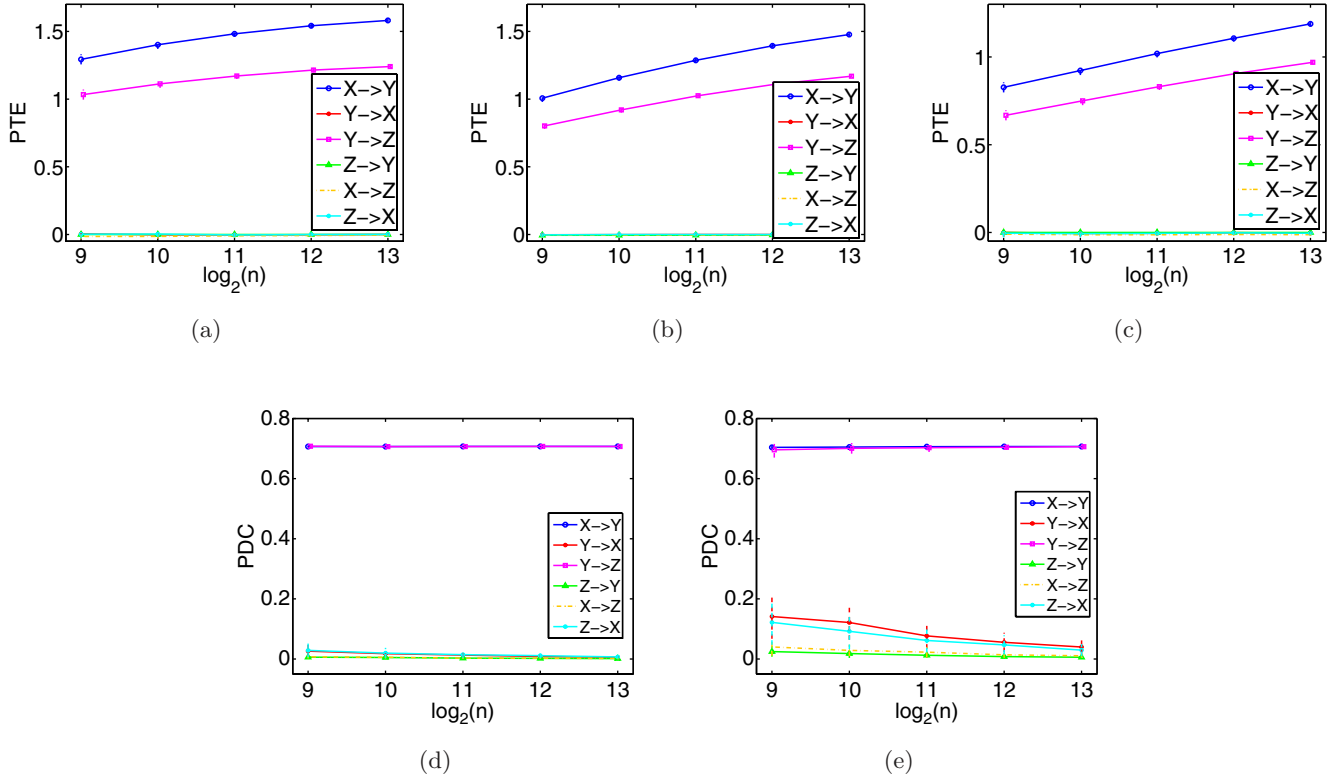


Fig. 1. (a) Mean estimated values and standard deviation (as error bars) of PTE versus  $\log_2 n$  from 100 realizations of system S1, for  $m = 1$  and  $k = 2$ . In (b) and (c), as in (a) but for  $m = 1, k = 10$ , and  $m = 2, k = 2$ , respectively. In (d) and (e), as in (a) but for PDC using  $P = 1$  and  $P = 2$ , respectively.

and 2(b)]. However, for the nonlinear flow of system S3, a larger time series is required to obtain significantly positive PTE values for the correct direct causal effects and relatively small variance across the 100 realizations.

### 3.2. Physiological data

We apply PTE and PDC to six extracranial EEG recordings from six epileptic patients to assess the information flow among brain areas during the

propagation of the epileptic activity, i.e. at the preictal, ictal and postictal states. The five EEG records are from generalized tonic clonic seizures (denoted as A to E), whereas the other EEG record, denoted F, is from left posterior temporal lobe seizure. Each EEG record covers at least 3 h prior to seizure onset and extends into the postictal period. The EEG data were high-pass filtered at 0.3 Hz and low-pass filtered at 40 Hz and were further down-sampled to 100 Hz (initially recorded at 256 Hz). To attain better source derivation at small cortical

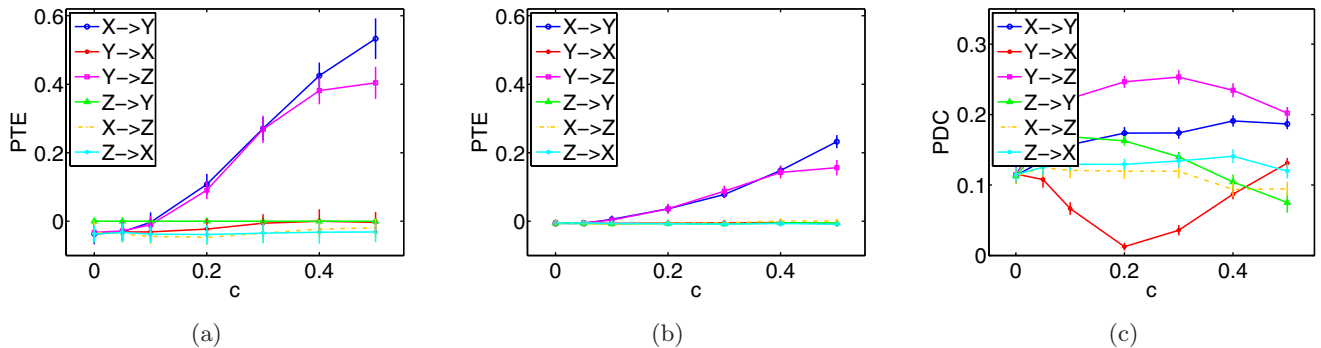


Fig. 2. (a) Mean estimated values and standard deviation (as error bars) of PTE versus  $c$  from 100 realizations of system S2, for  $n = 512, m = 2$  and  $k = 2$ . (b) As in (a) but for  $k = 10$ . (c) As in (a) but for PDC,  $n = 8192$  and  $P = 2$ .

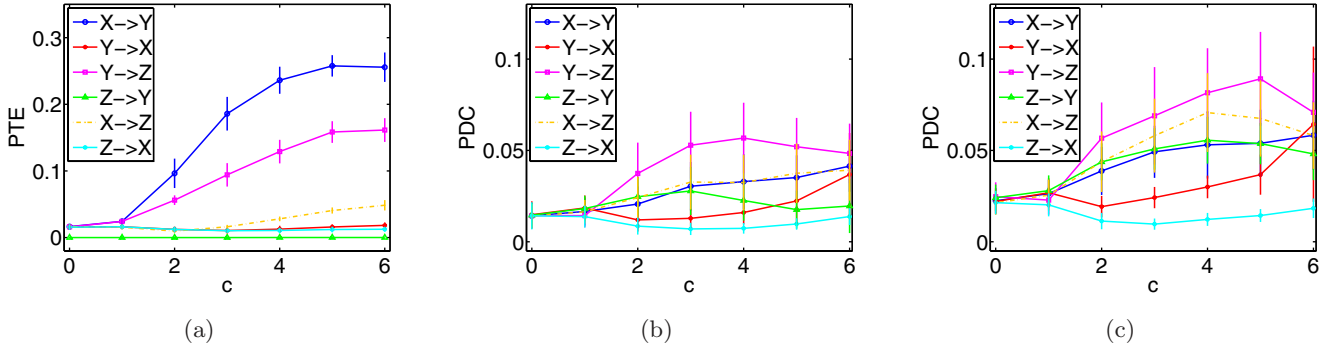


Fig. 3. (a) Mean estimated values and standard deviation (as error bars) of PTE versus  $c$  from 100 realizations of system S3, for  $n = 8192$ ,  $m = 3$  and  $k = 10$ . (b) and (c) are as in (a) but for PDC and for  $P = 3$  and  $P = 6$ , respectively.

regions, for each EEG channel, the mean EEG of the four neighboring channels is subtracted. In this study, we consider four channels (montage system 10–20) from the following brain areas: left frontal (F3), right frontal (F4), left temporal (T7) and right temporal (T8). We restrict the analysis to only four channels in order to keep the dimension low.

The measures are calculated on nonoverlapping consecutive EEG segments of 30 sec for all channel pair combinations. PDC is the average for frequencies from 1 to 30 Hz with step 1 Hz. For the order in PDC, we tested for  $P = 5, 6, 10, 20$  on one patient and found only a slight increase of PDC with  $P$ , which does not affect the detected direction of causal effects among the pairs of channels. On the other hand, PTE turns out to be more sensitive on the choice of  $m$ . Setting  $h = 5$ ,  $\tau = 5$  and  $m = 3, 5, 10$ , we found that PTE tends to decrease with the increase of  $m$ , and for  $m = 3$  the

causal effects between the pairs of channels at the two directions differed most, while for larger  $m$  the PTE decreased in both directions down to about the same level. We set  $k$  to 10 and 20 neighbors and found no significant effect on PTE, which is in agreement with the results of the simulation study. We tested for a range of  $m$  and  $P$  values as the simulation study showed that both PTE and PDC are sensitive to  $m$  and  $P$ , respectively. However, we found that the estimation of PTE for  $m = 10$  is unstable, which sets an upper bound for  $m$  in this data setting.

We made the calculations to all patients using  $m = 3$  and 5 for PTE ( $k = 10$ ) and  $P = 6$  and 20 for PDC. In all cases, PTE indicated the increase of information flow during the ictal and postictal states [see Figs. 4(a)–4(c) for patient A, B, C and  $m = 3$ ], while PDC does not produce this feature [see Figs. 4(d)–4(f) for  $P = 6$ ]. Also, in the preictal

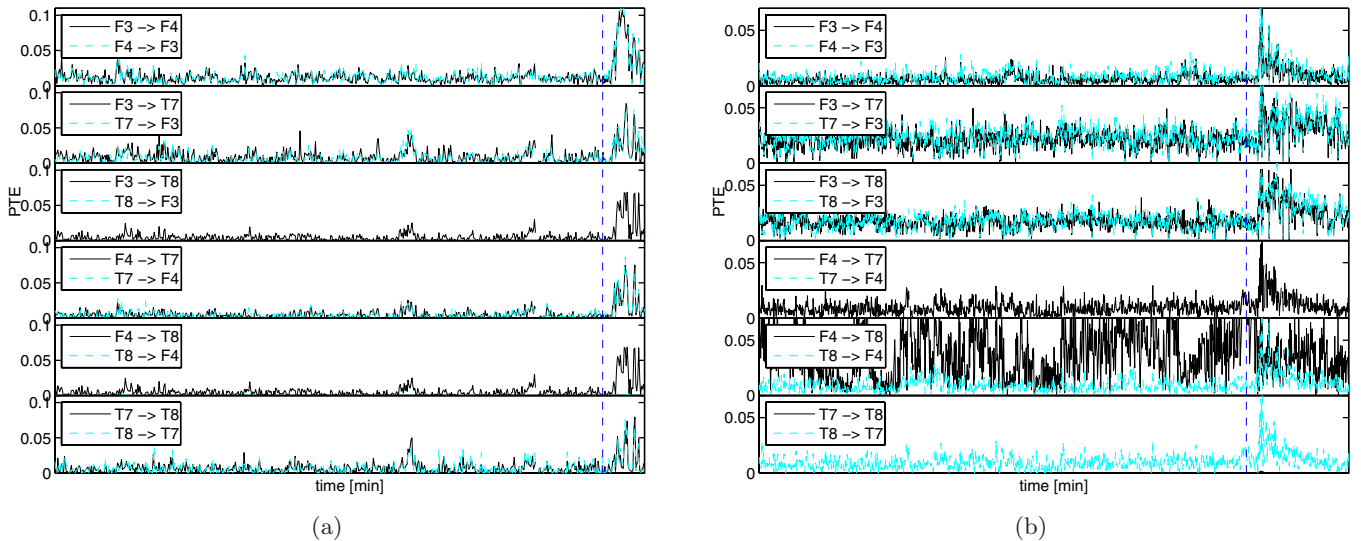


Fig. 4. (a)–(c) Estimated values of PTE for the first three records (A–C) for  $m = 3$  and  $k = 10$ . (d)–(f) Estimated values of PDC for the same records (A–C) for  $P = 6$ . The dotted vertical line indicates the seizure onset.

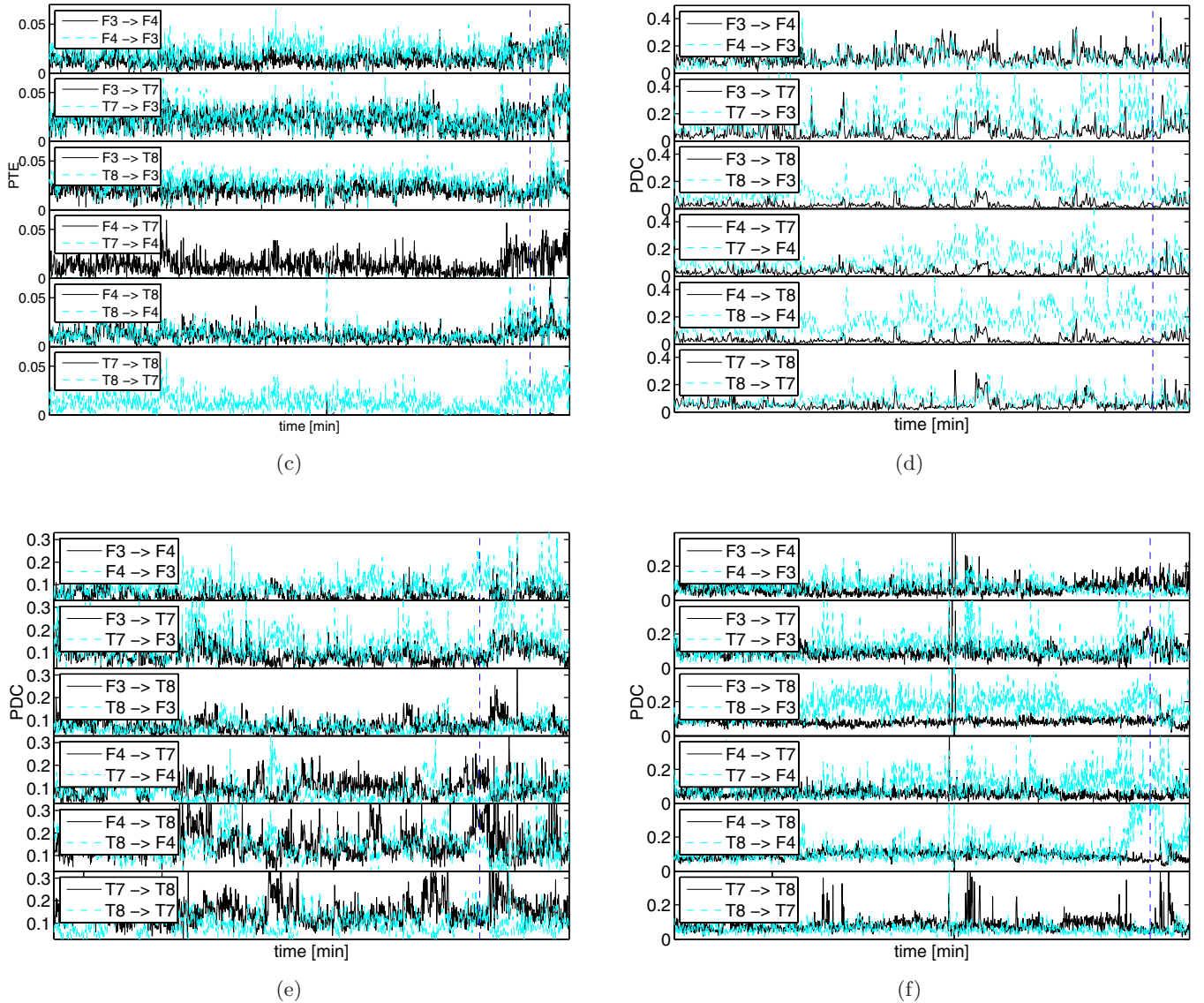


Fig. 4. (Continued)

state PTE and PDC do not indicate the same causal effects; e.g. for record A, PDC indicates driving of T7 and T8 on F3 and F4, respectively, and bidirectional interaction among all pairs of channels while PTE indicates weak bidirectional causal effect for F3 versus F4, F3 versus T7 and T7 versus T8 [see Figs. 4(a) and 4(d)]. Both measures vary much across the episodes and channels, and they are positive (at larger or smaller scales), suggesting the existence of bidirectional causal effects among the different brain areas. This, however, remains to be verified rigorously by statistical significance testing and inclusion of other causality measures. Both measures seem to be insufficient in detecting a precursor of the seizure onset, as no changes in the information flow are detected.

#### 4. Discussion

In this study, the identification of the interdependencies of coupled systems represented by observed time series was addressed. A nonlinear causality measure, partial transfer entropy, has been presented and was compared to a standard linear one, partial directed coherence. Simulations on a linear coupled system showed that PTE can detect causal effects as good as PDC even for small data sizes, whereas for nonlinear coupled systems PTE performs properly while PDC generally fails. However, PTE seems to be more sensitive to the embedding dimension  $m$  than PDC is to the model order  $P$  because a large  $m$  implies the estimation of high-dimensional distributions, which requires

larger data sets. The results of the simulations suggest that the parameter  $k$  is not crucial in the implementation of PTE, which is in agreement with other works [Kraskov *et al.*, 2004; Papana & Kugiumtzis, 2009].

The situation of having to use a large  $m$  in conjunction with limited data size may give rise to unreliable estimation of PTE, whereas this is not the case for PDC and a large  $P$ . This actually is the problem of estimating joint entropies and joint distributions at a high-dimensional state space. Recently, in [Vakorin *et al.*, 2009], PTE was introduced to derive directed connections between nodes (time series) of a network. They estimated the entropies in PTE with correlation sums and used only very small  $m$ . In our approach, we estimated the entropy terms using nearest neighbors and obtained better estimates at moderate to high dimensions, so that we can trade better system complexity and dimensionality.

For the application to six epileptic EEG records, we could obtain robust estimation of PTE for  $m = 5$  and four variables (the left/right temporal and frontal channels). Though there were variations in PTE with  $m$ , PTE was always at a higher level during ictal and postictal state for all six patients and channel combinations. We could not obtain this feature with PDC regardless of the magnitude of  $P$ . For the preictal state, both measures varied with patient and channel pairs, so the results were inconclusive as to the information flow hours to minutes before the seizure onset. To assess the effectiveness of the measures in detecting direct information flow, further investigation is needed on the parameter setting, in particular for PTE, as well as the model mis-specification, as only selected brain areas have been used in this study. Recent studies have given evidence that nonlinear measures have larger discriminating power in EEG analysis [Andrzejak *et al.*, 2011], and that brain connectivity mapping should be formed based only on direct causal effects [Gourevitch *et al.*, 2006]. Thus, the development of nonlinear direct causality measures, as the measure of PTE proposed here, may have a positive impact in EEG analysis (e.g. seizure prediction and epileptic focus localization) and complex system analysis in general.

## References

Andrzejak, R. G., Chicharro, D., Lehnertz, K. & Mormann, F. [2011] "Using bivariate signal analysis to

- characterize the epileptic focus: The benefit of surrogates," *Phys. Rev. E* **83**, 046203.
- Baccala, L. & Sameshima, K. [2001] "Partial directed coherence: A new concept in neural structure determination," *Biol. Cybern.* **84**, 463–474.
- Blinowska, K. J., Ku, R. & Kamiski, M. [2004] "Granger causality and information flow in multivariate processes," *Phys. Rev. E* **70**, 050902.
- Chen, Y., Bressler, S. L. & Ding, M. [2006] "Frequency decomposition of conditional Granger causality and application to multivariate neural field potential data," *J. Neurosci. Meth.* **150**, 228–237.
- Gourevitch, B., Bouquin-Jeannes, R. & Faucon, G. [2006] "Linear and nonlinear causality between signals: Methods, examples and neurophysiological applications," *Biol. Cybern.* **95**, 349–369.
- Guo, S., Seth, A. K., Kendrick, K., Zhou, C. & Feng, J. [2008] "Partial Granger causality — Eliminating exogenous inputs and latent variables," *J. Neurosci. Meth.* **172**, 79–93.
- Kraskov, A., Stögbauer, H. & Grassberger, P. [2004] "Estimating mutual information," *Phys. Rev. E* **69**, 066138.
- Papana, A. & Kugiumtzis, D. [2008] "Detection of directionality of information transfer in nonlinear dynamical systems," *Topics on Chaotic Systems, Selected Papers from CHAOS 2008 Int. Conf.*, 3–6 June, Chania (World Scientific, Singapore), pp. 251–264.
- Papana, A. & Kugiumtzis, D. [2009] "Evaluation of mutual information estimators for time series," *Int. J. Bifurcation and Chaos* **19**, 4197–4215.
- Schelter, B., Winterhalder, M., Eichler, M., Peifer, M., Hellwig, B., Guschlbauer, B., Lucking, C. H., Dahlhaus, R. & Timmer, J. [2006a] "Testing for directed influences among neural signals using partial directed coherence," *J. Neurosci. Meth.* **152**, 210–219.
- Schelter, B., Winterhalder, M. & Timmer, J. [2006b] *Handbook of Time Series Analysis: Recent Theoretical Developments and Applications* (Wiley-VCH, Berlin).
- Schreiber, T. [2000] "Measuring information transfer," *Phys. Rev. Lett.* **85**, 461–464.
- Takahashi, D. Y., Baccala, L. A. & Sameshima, K. [2007] "Connectivity inference between neural structures via partial directed coherence," *J. Appl. Stat.* **34**, 1259–1273.
- Vakorin, V. A., Krakovska, O. A. & McIntosh, A. R. [2009] "Confounding effects of indirect connections on causality estimation," *J. Neurosci. Meth.* **184**, 152–160.
- Vlachos, I. & Kugiumtzis, D. [2010] "Non-uniform state space reconstruction and coupling detection," *Phys. Rev. E* **82**, 016207.